Supplementary Information

Al Doping-Induced Electron Delocalization of Co_3O_4 Boosting Efficient Peracetic Acid Activation for Water Decontamination

Quan Wang[a], Hao Chen[a,*], Zhaodi Zhang[a], Jiaxuan Wei[a], Wenjun Gao[a], Boqing Zhang[a], Sha Yu[a], Yuanzhen Zhou[a,b]

a School of Chemistry and Chemical Engineering, Xi'an University of Architecture and Technology, Xi'an, 710055, China

b Engineering Research Center of Low-Carbon Energy Efficient Utilization, Universities of Shaanxi Province, Xi'an, 710055, China

Corresponding addresses: School of Chemistry and Chemical Engineering, Xi'an University of Architecture and Technology, No. 13, Yanta Road, Xi'an, Shaanxi Province, China.

Corresponding author email: chenhao@xauat.edu.cn (H. Chen)

Text S1. Chemicals and reagents.

Hydrogen peroxide (H_2O_2), acetic acid (CH_3COOH), N,N-diethyl-p-phenylenediamine (DPD), potassium iodide (KI), methyl phenyl sulfoxide (PMSO), methyl phenyl sulfone ($PMSO_2$), tetracycline (TC). HPLC-grade acetonitrile was obtained from TEDIA Co., Ltd (USA). Additional chemicals, including metal nitrates (> 98%, AR), aluminum isopropoxide (> 98%, AR), Na_2CO_3 (> 99.8%, AR), NaOH (> 96%, AR), ethanol (> 98%, AR), ethyl levulinate (EL, > 99%, AR), n-butylamine (> 99.8%, AR), and alcohols (> 98%, AR). potassium thiocyanate (KSCN), hydrochloric acid (HCl), sulfuric acid (H_2SO_4), phosphoric acid (H_3PO_4), furfuryl alcohol (FFA), 2, 4-hexadiene (2,4-HD), naproxen (NAP), 4-chlorobenzoic acid (p-CBA) and tert-butyl alcohol (TBA), were sourced from Aladdin Industrial Corporation (Shanghai, China). Sodium borohydride (NaBH4), humic acid (HA), sodium chloride (NaCl), sodium carbonate (Na_2CO_3), sodium bicarbonate ($NaHCO_3$), disodium hydrogen phosphate (Na_2HPO_4), 1, 10-phenanthroline (Phen), $K_2Cr_2O_7$, and acetone were acquired from Sinopharm Chemical Reagent Co. Ltd. All chemicals and solvents were used as received without further purification, and solutions were prepared using deionized water with a resistivity of >18.2 MΩ • cm, produced by a Millipore Milli-Q system.

Text S2. Preparation of PAA Stock Solution.

The PAA solution was synthesized with using CH_3COOH to react with H_2O_2 under the catalysis of H_2SO_4. Firstly, 20 mL CH_3COOH was mixed with 10 mL H_2O_2. And then, 1 mL H_2SO_4 was added into the mixture and stirred evenly. Finally, the obtained mixture was aged and stocked in the refrigerator at 4°C.

Text S3. Determination of PAA concentration.

N,N'-diethyl-p-phenylenediamine (DPD) colorimetric method. The total concentration of PAA and H_2O_2 was first determined by iodometric titration[1]. Although the PAA stock solution was stored at 4 °C, its concentration required regularly calibrated. In the iodometric methods, potassium iodide was reacted with peroxides to liberate iodine, which was then titrated with sodium thiosulfate. The H_2O_2 concentration was separately determined by titration with potassium permanganate under acidic conditions. The PAA concentration was calculated by subtracting the concentration from the total peroxide concentration. For residual PAA quantification in experimental samples, a colorimetric method was employed. Potassium iodide (KI) and DPD were used to detect PAA concentration. Briefly. 0.5 mL of KI and 0.5 mL of DPD were added to a sample solution in a 10 mL colorimeter tube. The liberated iodine reacted with DPD to form a pink-colored species, the absorbance of which was measured at 515 nm. The absorbance was directly proportional to the PAA concentration.

Text S4. Characterization Methods.

High-resolution transmission electron microscopy (HRTEM) combined with a high-angle annular dark-field (HAADF) detector and energy-dispersive X-ray spectroscopy (EDS) was performed on a FEI Talos F200x instrument to analyze the structural and compositional features of the catalysts. X-ray powder diffraction (XRD) analysis was conducted using a Bruker D8-Advance diffractometer with Cu-Kα radiation, scanning from 10° to 80° to characterize the crystal structure of the catalysts. Surface chemical composition, elemental content, and valence states were analyzed via X-ray photoelectron spectroscopy (XPS) using a Thermo ESCALAB instrument equipped with Al-Kα radiation (hν = 1486.6 eV). The C1s peak at 284.8 eV was used for calibration, and spectral analysis was performed using Casa XPS software.

Text S5. Analytical methods.

The high-performance liquid chromatography (HPLC) detection conditions for tetracycline (TC) are as follows: the mobile phase consists of an acetonitrile and 0.1% formic acid in the ratio of 30:70 as mobile phase, the flow rate was 0.3 mL/min, and the temperature of the column oven was 30 ℃ and the detection wavelength was 360 nm.

The degradation kinetic curves of TC were fitted by the pseudo-first-order kinetic model:

$$\ln\left(\frac{C_t}{C_0}\right) = -k_{obs}t$$

Where C_0 (mg/L) and C_t (mg/L) correspond to the concentration of TC at the initial state and t (min) degradation time, respectively; kobs is the degradation rate constant.

Electron paramagnetic resonance (EPR) measurements were conducted on a Bruker A300 spectrometer (Germany) to detect reactive radicals generated. Three spin-trapping agents were employed: 5,5-dimethyl-1-pyrroline N-oxide (DMPO, > 99%, Aladdin), 2,2,6,6-tetramethyl-4-piperidinol (TEMP, > 98%, Aladdin). For DMPO and TEMP, the operating conditions were as follows: center field 3460 G, sweep width 100 G, microwave frequency 9.71 GHz, microwave power 19.71 mW, modulation frequency 100 kHz, modulation amplitude 1.0 G, and sweep time 83.97 s. Raman spectra were recorded using a LabRAM Aramis Raman spectrometer (Horiba Scientific) with a 532 nm Ar laser. Powdered samples were pressed into a sample holder and placed in a custom-built reaction cell for in situ Raman measurements. In-situ ATR-FTIR spectra were recorded on a Bruker TENSOR II FTIR spectrometer equipped with a dedicated ATR accessory. The spectra were collected in the range of 1000–4000 cm^{-1} to monitor the evolution of PAA on the catalyst surface and to analyze the functional groups of the catalysts.

Text S6. Electrochemical tests.

Electrochemical measurements were conducted using a CHI760E electrochemical workstation equipped with a standard three-electrode electrochemical cell. The working electrode was prepared mixing 5 mg of catalyst, 1 mL of ultrapure water, and 50 μL of Nafion solution (5 wt%). 200 μL of the catalyst ink was uniformly coated on the carbon paper (1 cm × 1 cm) and dried at room temperature. The obtained carbon paper was taken with an electrode clamp and acted as the working electrode. The Pt and Ag/AgCl electrodes (saturated KCl solution) served as the counter electrode and reference electrode, respectively. Specifically, Na_2SO_4 (0.5 M) was utilized as the electrolyte. CV curves of different catalysts were performed at a scan rate of 10 $mV \cdot s^{-1}$.

Text S7. DFT calculations.

All density functional theory (DFT) calculations were performed using the Cambridge Sequential Total Energy Package (CASTEP). The generalized gradient approximation (GGA) with the Perdew–Burke–Ernzerhof (PBE) functional was employed to describe electron exchange and correlation. Electron–ion interactions were treated using the projector-augmented wave (PAW) method, with a plane-wave cutoff energy set to 450 eV. Dispersion corrections were incorporated via the DFT-D3 method. Geometry optimizations were considered converged when the energy change between electronic steps fell below 1×10^{-5} eV and the maximum force on any atom was less than 0.03 eV/Å. A (1×1×1) Monkhorst–Pack k-point mesh was used for sampling the Brillouin zone of the slab model, which included a 15 Å vacuum layer. During structural relaxation, all atomic positions and in-plane cell vectors were fully relaxed, while the cell vector along the z-axis remained fixed.

The adsorption energy (E_{ads}) of PAA on different surface structures was defined as:

$$E_{ads} = E_{total} - E_{surface} - E_{PAA}$$

where E_{total} is the total energy of the slab with an adsorbed PAA molecule, $E_{surface}$ is the energy of the clean slab, and E_{PAA} is the energy of an isolated PAA molecule. A more negative E_{ads} corresponds to stronger adsorption.

The charge density difference ($\Delta\rho$) was computed to visualize electron redistribution upon adsorption:

$$\Delta\rho=\rho_{AB}-\rho_{A}-\rho_{B}$$

where ρ_{AB} is the total charge density of the adsorbed system, and ρ_A and ρ_B represent the charge densities of the isolated slab and the PAA molecule, respectively.

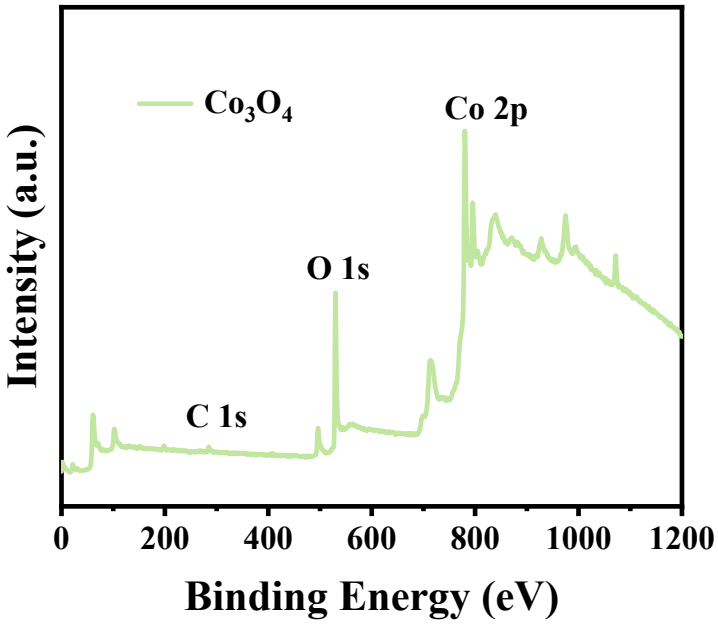

Fig. S1 XPS Full Spectrum of Co_3O_4.

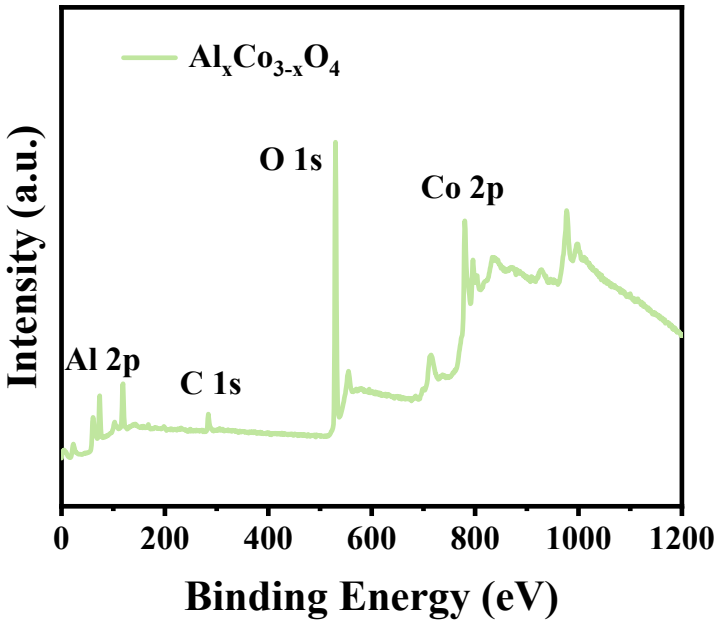

Fig. S2 XPS Full Spectrum of $Al_xCo_{3-x}O_4$.

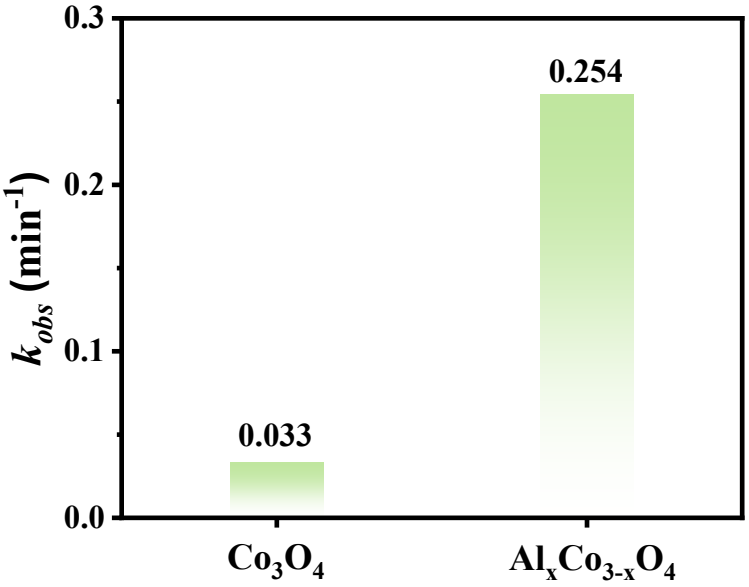

Fig. S3 The observed rate constants (k_{obs}) for different materials.

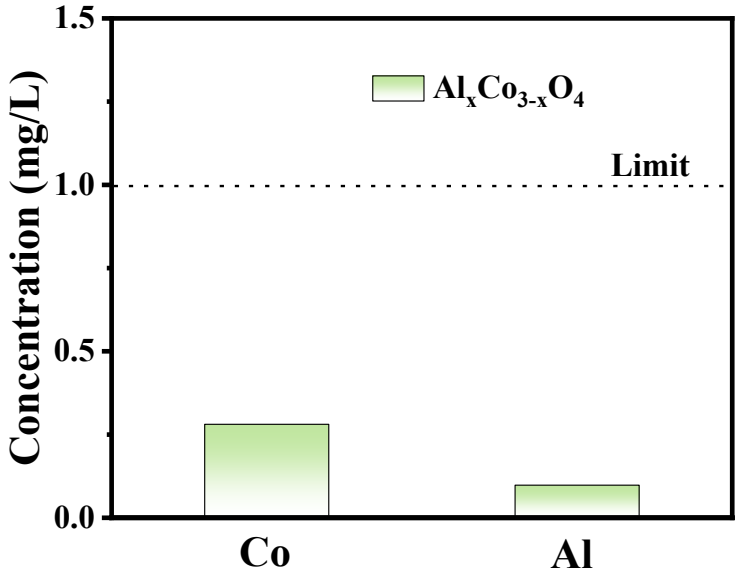

Fig. S4 Leaching of metal ions from $Al_xCo_{3-x}O_4$.

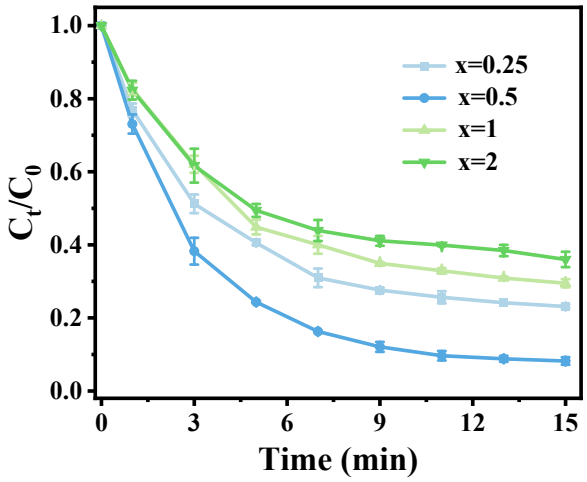

Fig. S5. (a) PAA activation performance of $Al_xCo_{3-x}O_4$ samples with different nominal Al contents (x = 0.25, 0.5, 1, 2) under identical reaction conditions. Experimental conditions: $[Al_xCo_{3-x}O_4]$ = 0.2 g/L, $[PAA]_0$ = 0.4 mM, $[TC]_0$ = 10 μM, $[pH]_0$ = 7.

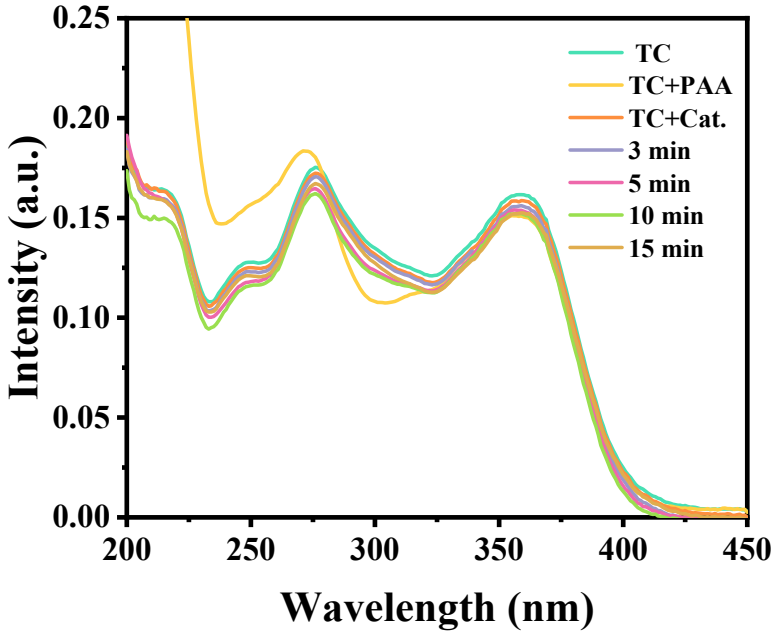

Fig. S6 UV-vis absorption spectra of $Al_xCo_{3-x}O_4$ and PAA with TC during the degradation process

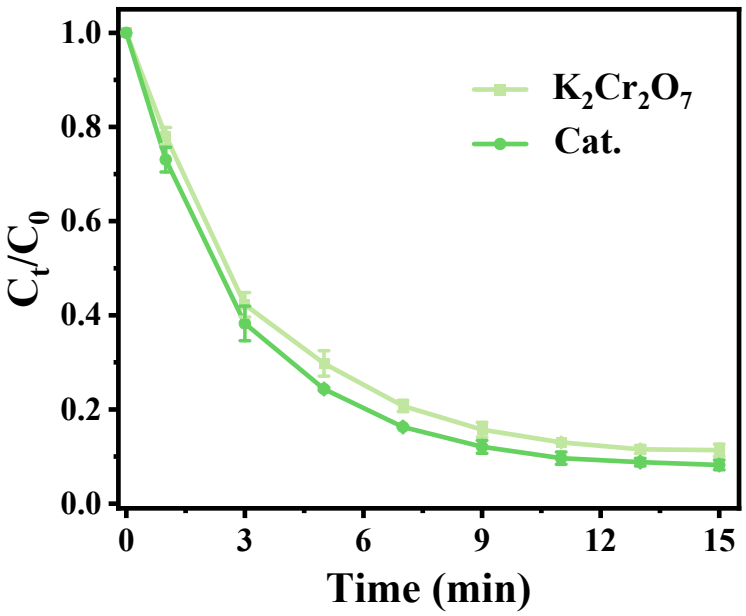

Fig. S7 Degradation efficiency of TC via PAA activation by different catalysts with and without adding 1 mM of $K_2Cr_2O_7$. Reaction conditions: $[Al_xCo_{3-x}O_4]_0$=0.2 g/L; $[PAA]_0$=0.4 mM; $[TC]_0$=10 μM; $[K_2Cr_2O_7]_0$=1 mM; $[pH]_0$=7; temperature = 25 °C.

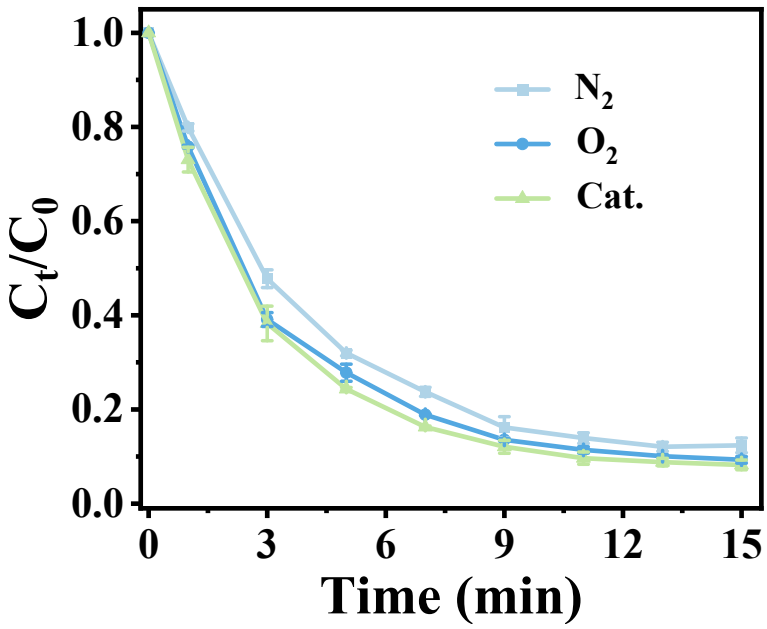

Fig. S8 Degradation rates of TC under different atmospheric conditions. Reaction conditions: $[Al_xCo_{3-x}O_4]_0$=0.2 g/L; $[PAA]_0$=0.4 mM; $[TC]_0$=10 μM; $[pH]_0$=7; temperature = 25 °C.

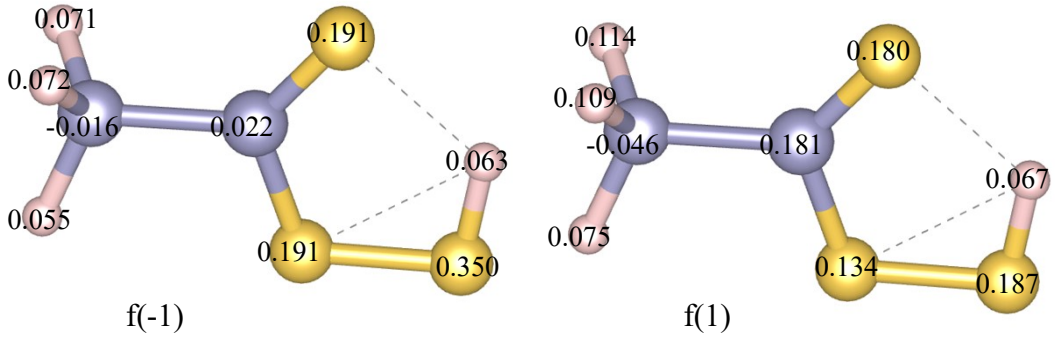

Fig. S9 Charge distribution of PAA under electron gain and loss.

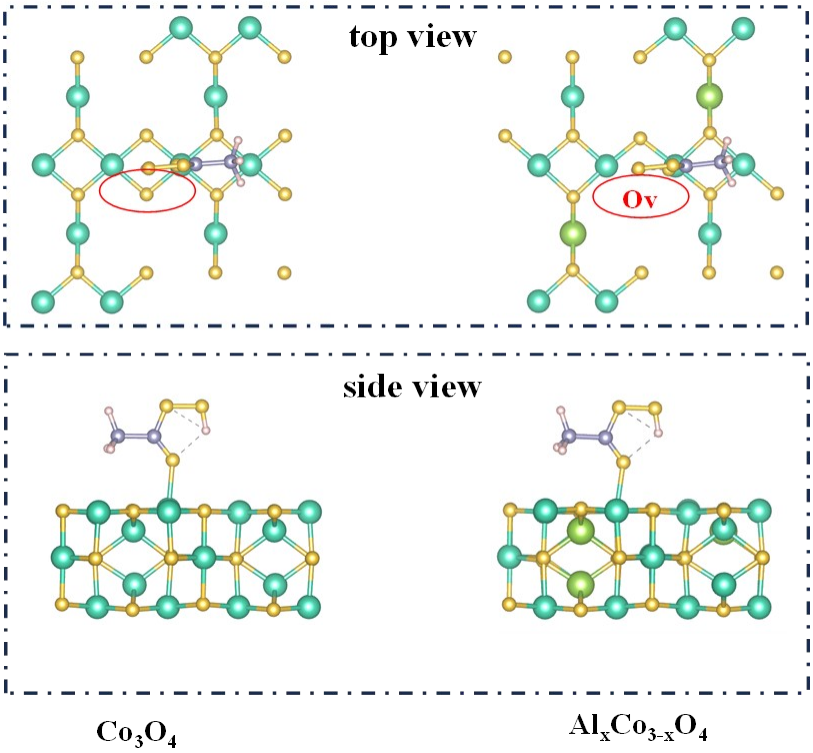

Fig. S10. Optimized adsorption configuration of PAA on the Co_3O_4 and $Al_xCo_{3-x}O_4$ surface: (a) top view, (b) side view.

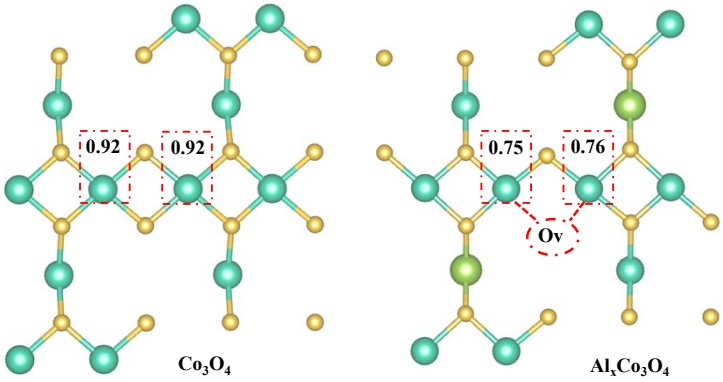

Fig. S11 Bader charge distributions of Co_3O_4 and $Al_xCo_{3-x}O_4$.

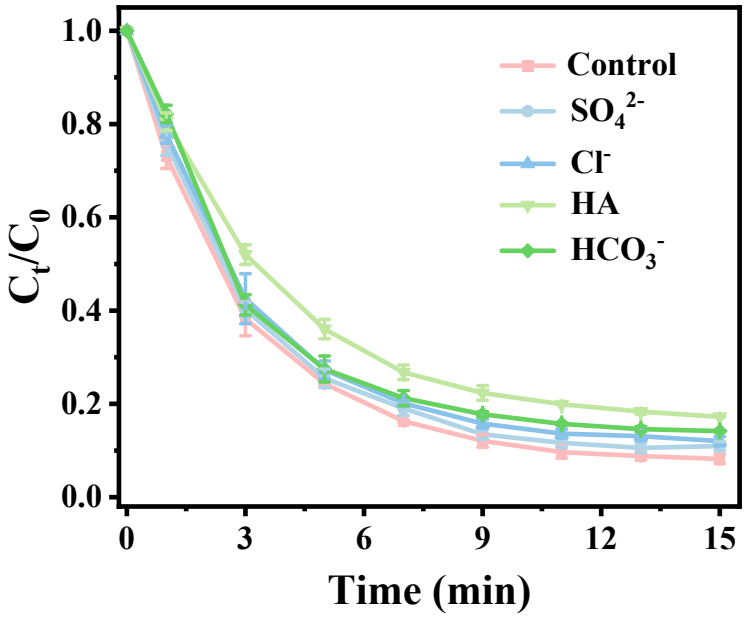

Fig. S12 Influence of Inorganic Anions on Tetracycline (TC) Removal Process, (Experiment:conditions:

$[Al_xCo_{3-x}O_4]_0$=0.2 g/L; $[PAA]_0$=0.4 mM; $[TC]_0$=10 μM; $[pH]_0$=7; temperature = 25°C.

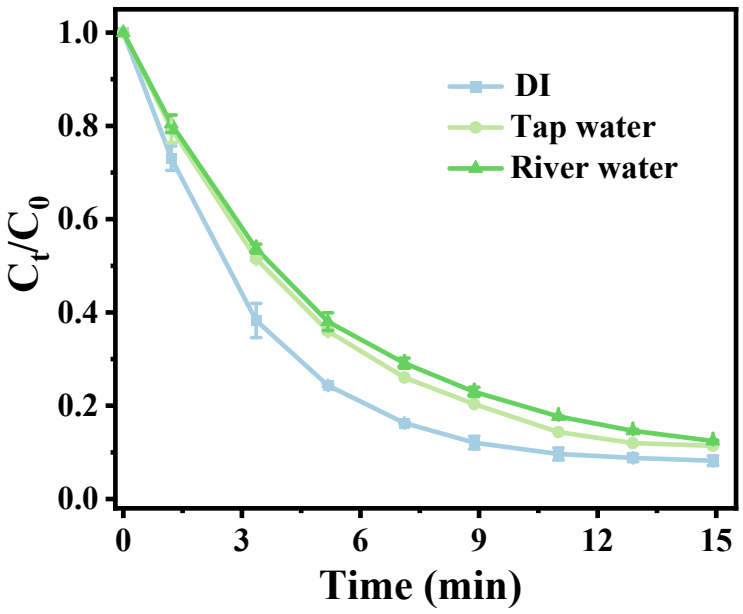

Fig. S13 Effect of different water on TC degradation. (Experiment:conditions: $[Al_xCo_{3-x}O_4]_0$=0.2 g/L; $[PAA]_0$=0.4 mM; $[TC]_0$=10 μM; $[pH]_0$=7.

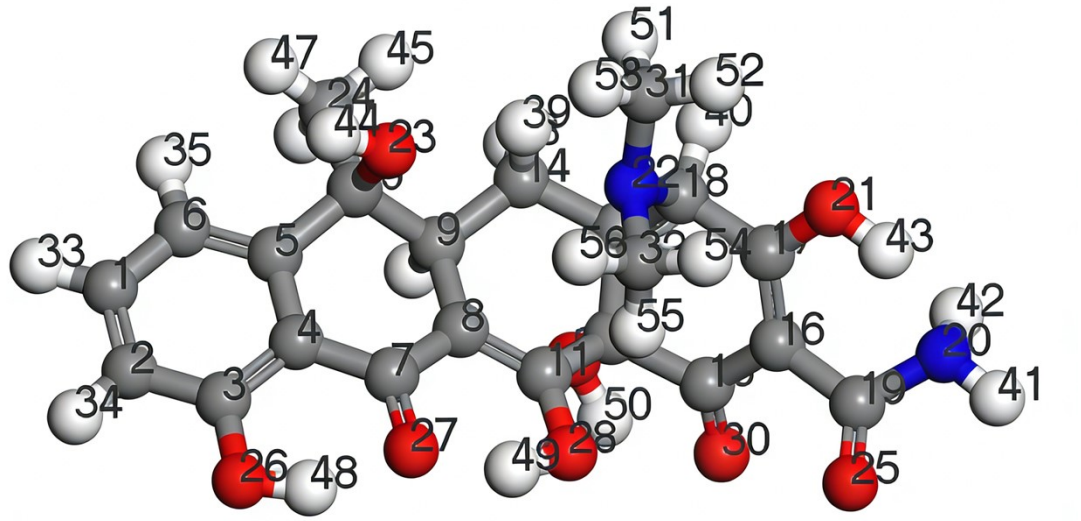

Fig. S14 Atom Numbering Scheme of the Tetracycline (TC) Molecule.

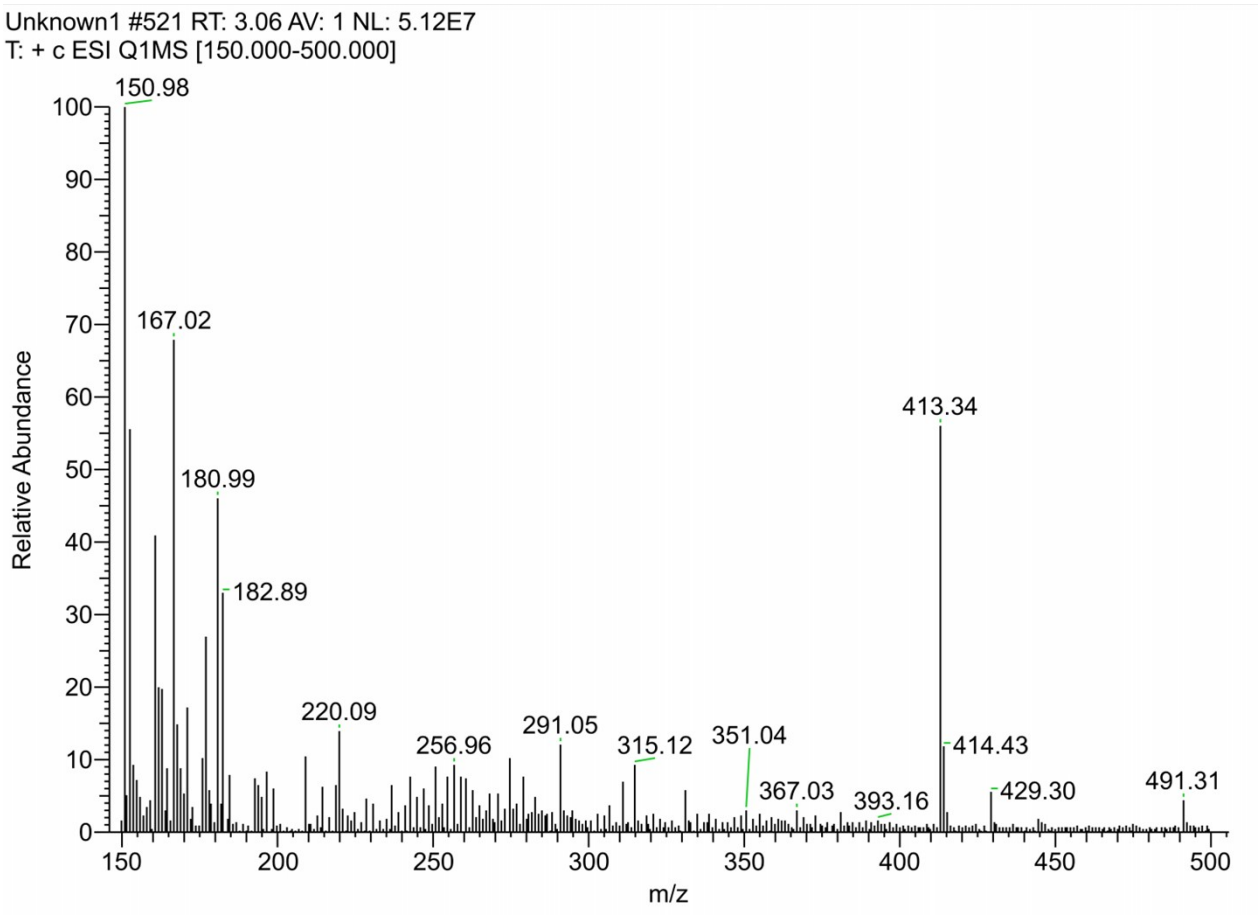
Unknown1 #521 RT: 3.06 AV: 1 NL: 5.12E7
T: + c ESI Q1MS [150.000-500.000]
150.98
167.02
180.99
182.89
220.09
256.96
291.05
315.12
351.04
367.03
393.16
413.34
414.43
429.30
491.31
Relative Abundance
m/z

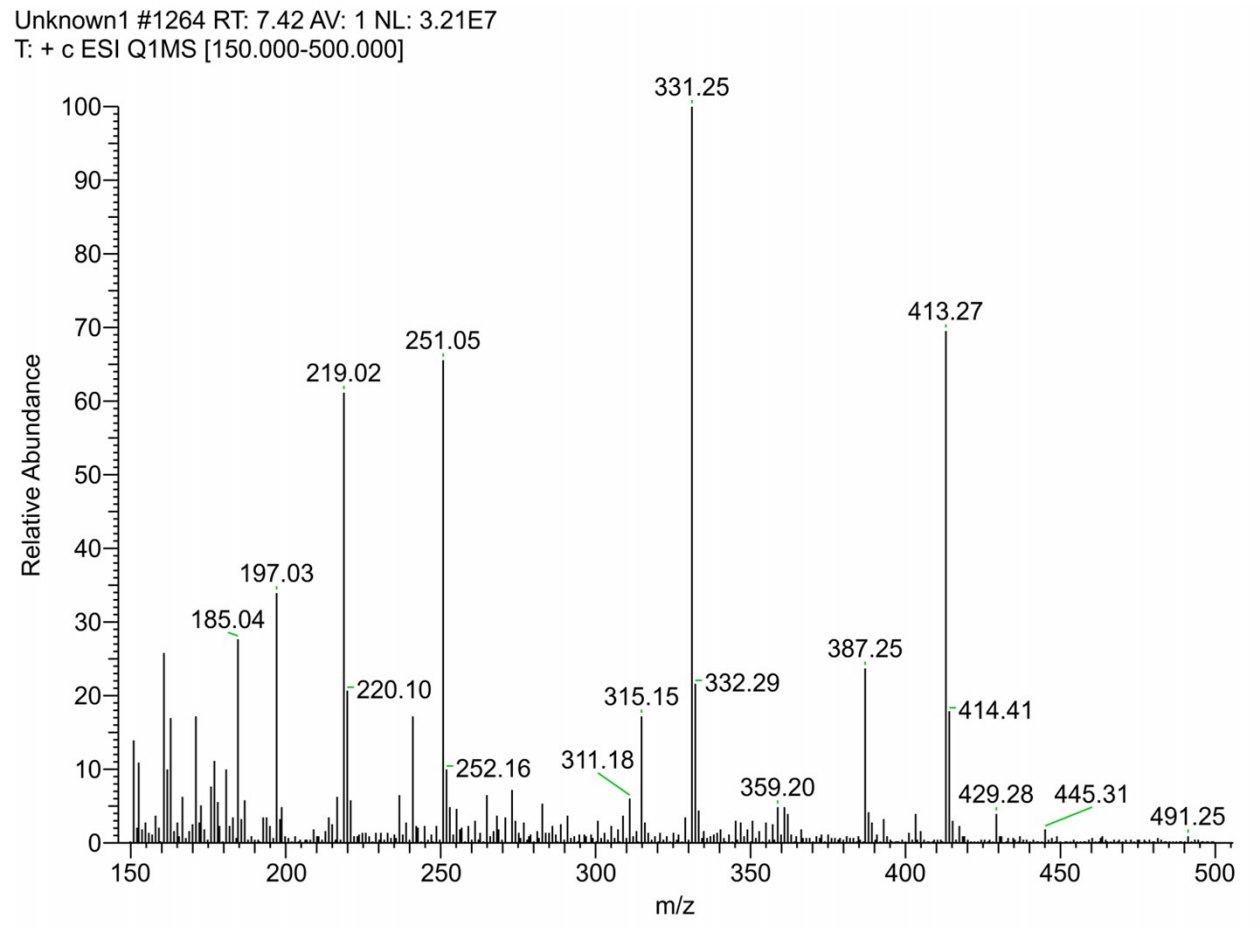
Unknown1 #1264 RT: 7.42 AV: 1 NL: 3.21E7
T: + c ESI Q1MS [150.000-500.000]
331.25
413.27
251.05
219.02
197.03
185.04
220.10
252.16
311.18
315.15
332.29
387.25
414.41
359.20
429.28
445.31
491.25
Relative Abundance
m/z

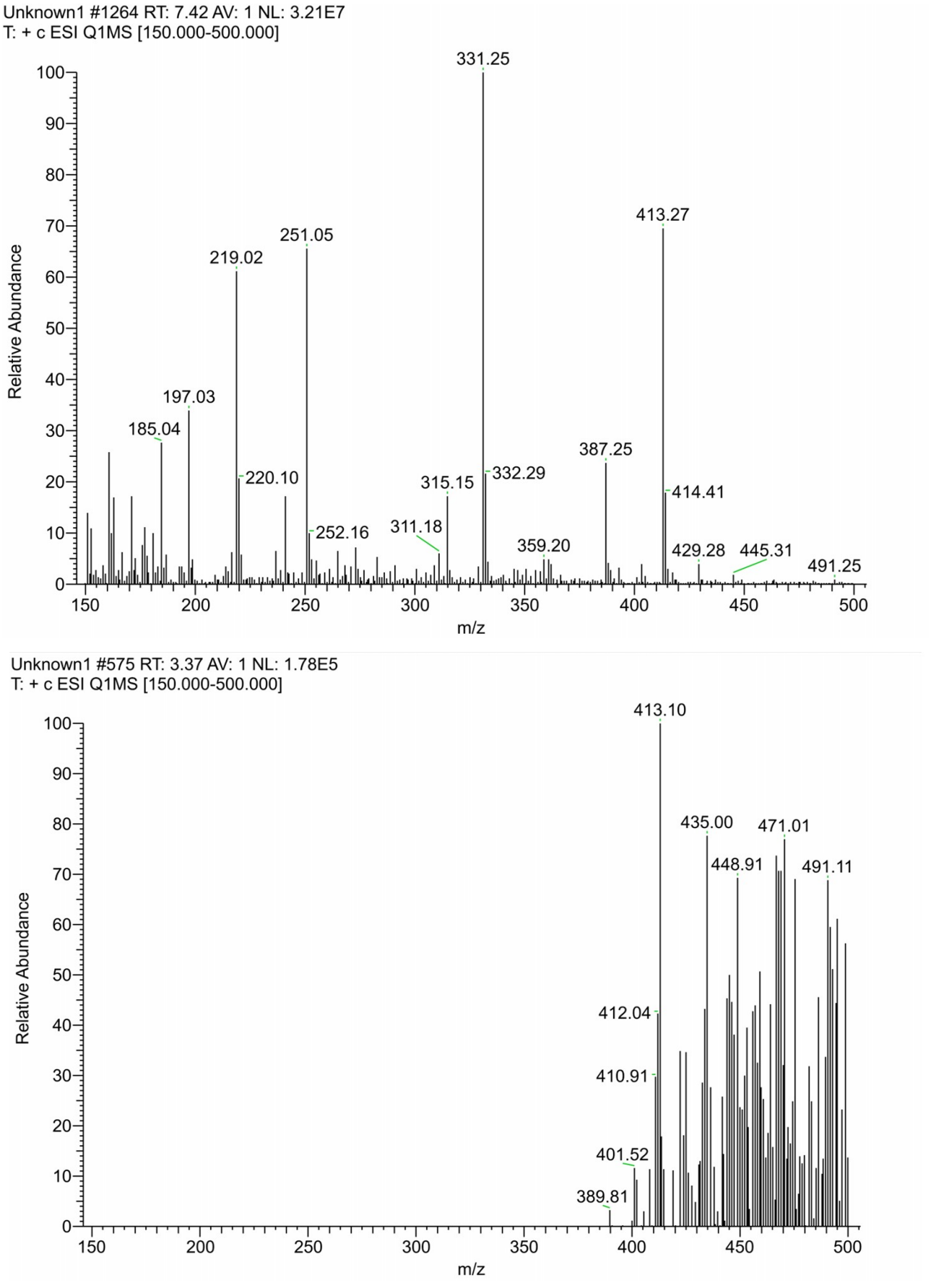

Fig. S11. gradation intermediates of TC $Al_xCo_{3-x}O_4$/PAA system determined by LC-MS.

Table S1. Standard curve of TC at different pH.

pH	R^2	linear equation
3	0.9992	Y=0.0337X-0.0003
5	0.9991	Y=0.0329X+0.0005
7	0.9994	Y=0.0303X+0.0068
9	0.9995	y=0.0310x−0.0009
11	0.9993	Y=0.0318X+0.0011

Table S2. Comparison of this work with other advanced oxidation processes.

Catalyst	Catalyst Dosage (mg/L)	Catalytic mode (mM)	Contaminant (μM)	$k_{obs}(min^{-1})$	Reference
$Al_xCo_{3-x}O_4$	200	400 PAA	10 TC	0.254	This work
pyrite	100	100 PAA	10 TC	0.123	[4]
zero valent iron	60	100 PAA	10 TC	0.039	[5]
π-COF	200	Photocatalytic	40 TC	0.085	[6]
Co-Fe-Cube	40	100 PAA	10 SMX	0.087	[7]
BNQDs-FCN	200	100 PAA	10 TC	0.084	[8]

Table S3. The main degradation intermediates in $Al_xCo_{3-x}O_4$/PAA/TC system.

Compounds	$[M+H]^+$ (m/z)	Structure
TC	445	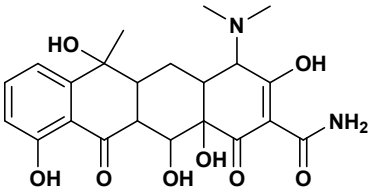
P1	434	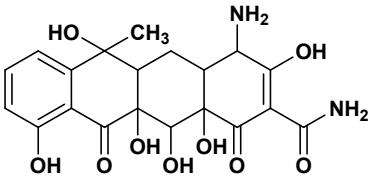
P2	411	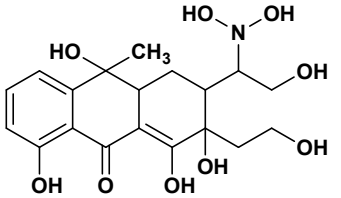
P3	336	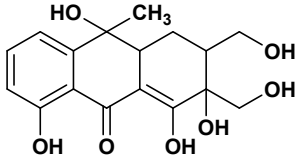
P4	491	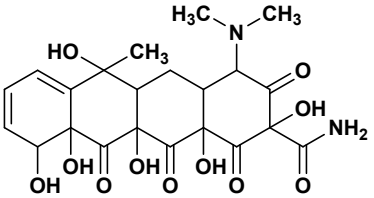
P5	435	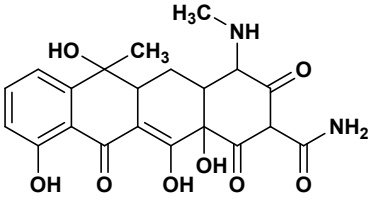
P6	413	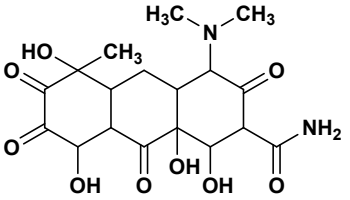
P7	429	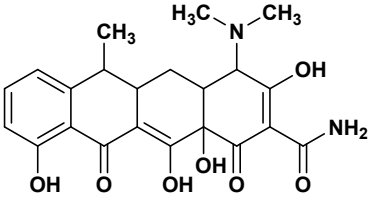

P8	414	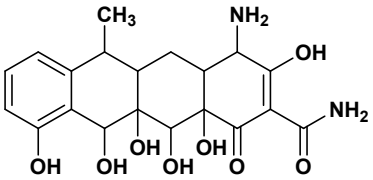
P9	401	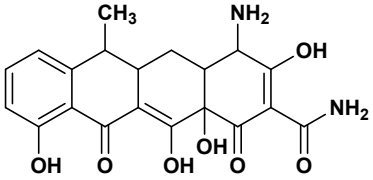
P10	218	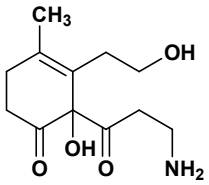
P11	167	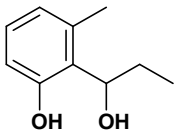
P12	197	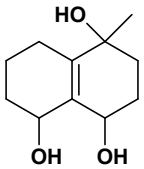

Table S6. Fukui Function Distribution at Different Sites in the Tetracycline Molecule.

Index	Electrophilic, f (-)	Nucleophilic, f (+)	Radical, f (0)
C (1)	0.012	0.041	0.027
C (2)	0.022	0.016	0.019
C (3)	0.015	0.029	0.022
C (4)	0.017	-0.006	0.005
C (5)	0.004	0.031	0.017
C (6)	0.026	0.006	0.016
C (7)	0.008	0.073	0.041
C (8)	0.014	-0.001	0.007
C (9)	-0.009	-0.008	-0.008
C (10)	-0.004	-0.01	-0.007
C (11)	0.005	0.06	0.032
C (12)	0	-0.007	-0.004
C 13)	-0.011	-0.012	-0.011
C (14)	-0.016	-0.01	-0.013
C (5)	-0.001	0.02	0.01
C (16)	0.022	0.003	0.012
C (17)	-0.002	0.044	0.021
C (18)	-0.019	-0.013	-0.016
C (19)	0.003	0.011	0.007
N (20)	0.002	0.003	0.002

O (21)	0.005	0.029	0.017
N (22)	0.099	-0.006	0.046
O (23)	-0.007	0.007	0
C (24)	-0.01	-0.011	-0.01
O (25)	0.026	0.025	0.026
O (26)	0.055	0.041	0.048
O (27)	0.023	0.06	0.041
O (28)	0.038	0.046	0.042
O (29)	0.019	0.021	0.02
O (30)	0.041	0.05	0.046
C (31)	-0.033	-0.016	-0.024
C (32)	-0.024	-0.011	-0.018
H (33)	0.04	0.049	0.045
H (34)	0.04	0.045	0.042
H (35)	0.035	0.039	0.037
H (36)	0.029	0.022	0.026
H (37)	0.037	0.03	0.034
H (38)	0.035	0.028	0.031
H (39)	-0.002	0.015	0.006
H (40)	0.037	0.031	0.034
H (41)	0.021	0.023	0.022
H (42)	0.011	0.011	0.011

H (43)	0.012	0.013	0.013
H (44)	0.014	0.013	0.014
H (45)	0.013	0.02	0.016
H (46)	0.017	0.016	0.017
H (47)	0.019	0.02	0.019
H (48)	0.012	0.012	0.012
H (49)	0.011	0.016	0.013
H (50)	0.015	0.016	0.015
H (51)	0.043	0.015	0.029
H (52)	0.069	0.024	0.047
H (53)	0.039	0.016	0.028
H (54)	0.069	0.028	0.049
H (55)	0.023	-0.016	0.004
H (56)	0.038	0.012	0.025

References

1 M. Cai, P. Sun, L. Zhang and C.-H. Huang, *Environ. Sci. Technol.*, 2017, **51**, 14217–14224.

2 Y. Ren, C. Liu, C. Ji, B. Lai, W. Zhang and J. Li, *J Hazard Mater*, 2024, **473**, 134639.

3 L. Zhang, J. Chen, T. Zheng, Y. Xu, T. Liu, W. Yin, Y. Zhang and X. Zhou, *Water Res*, 2023, **229**, 119462.

4 D. Xing, S. Shao, Y. Yang, Z. Zhou, G. Jing and X. Zhao, *Water Res*, 2022, **222**, 118930.

5 L. Zhang, J. Chen, Y. Zhang, Z. Yu, R. Ji and X. Zhou, *Appl. Catal. B: Environ*, 2021, **297**, 120475.

6 Z. Hu, Y. Wang, L. Wang, Q. Wang, Q. Zhang, F. Cui and G. Jiang, *Chem Eng J*, 2024, **479**, 147534.

7 Y. Cheng, Z. Wang, L. Cao, Z. Chen, Y. Chen, Z. Liu, J. Ma and P. Xie, *Appl. Catal. B: Environ*, 2024, **342**, 123409.

8 S. Li, Y. Yang, J. Niu, H. Zheng, W. Zhang, Y. K. Leong, J.-S. Chang and B. Lai, *Environ. Sci. Technol.*, 2024, **58**, 21871–21881.